High average power, widely tunable femtosecond laser source from red to mid-infrared based on an Yb-fiber-laser-pumped optical parametric oscillator

High average power, widely tunable femtosecond laser source from red to mid-infrared based on an Yb-fiber-laser-pumped optical parametric oscillator

Chenglin Gu,[1] Minglie Hu,*,[1] Limeng Zhang,[1] Jintao Fan,[1] Youjian Song,[1] Chingyue Wang,[1] and Derryck T. Reid[2]

[1]*Ultrafast Laser Laboratory, Key Laboratory of Opto-electronic Information Science and Technology of Ministry of Education, College of Precision Instruments and Opto-electronics Engineering, Tianjin University, Tianjin 300072, China*

[2]*Scottish Universities Physics Alliance (SUPA), Department of Physics, School of Engineering and Physical Sciences, Heriot-Watt University, Riccarton, Edinburgh EH14 4AS, UK*

**Corresponding author: huminglie@tju.edu.cn*

Received March 12, 2013; revised April 21, 2013; accepted April 22, 2013; posted April 24, 2013 (Doc. ID 186925); published May 21, 2013

We report on the highly efficient generation of widely tunable femtosecond pulses based on intracavity second harmonic generation (SHG) and sum frequency generation (SFG) in a MgO-doped periodically poled $LiNbO_3$ optical parametric oscillator (OPO), which is pumped by a Yb-doped large-mode-area photonics crystal fiber femtosecond laser. Red and near infrared from intracavity SHG and SFG and infrared signals were directly obtained from the OPO. A 2 mm $\beta-BaB_2O_4$ is applied for Type I ($oo \rightarrow e$) intracavity SHG and SFG, and then femtosecond laser pulses over 610 nm ~ 668 nm from SFG and 716 nm ~ 970 nm from SHG are obtained with high efficiency. In addition, the oscillator simultaneously generates signal and idler femtosecond pulses over 1450 nm ~ 2200 nm and 2250 nm ~ 4000 nm, respectively.

OCIS codes: (190.4970) Parametric oscillators and amplifiers; (320.7090) Ultrafast lasers.
http://dx.doi.org/10.1364/OL.38.001820

Femtosecond laser sources in visible, infrared, and mid-infrared ranges are of great importance in many applications including biophotonics, optical microscopy, and time-resolved spectroscopy [1,2]. Optical parametric oscillators (OPOs) or amplifiers (OPAs) pumped by femtosecond Ti:sapphire lasers have been the preferred source in the past for this range [3,4]. The first demonstration of a high-repetition-rate, femtosecond OPOs based on periodically poled $LiNbO_3$ (PPLN) pumped by a femtosecond Ti:sapphire laser is reported by Burr *et al.* [5]. Theoretical and experimental work on OPO with intracavity second harmonic generation (SHG) and sum frequency generation (SFG) was reported by Koch *et al.* [6] in detail. Nowadays, the rapid progress in ultrafast fiber lasers leads to the development of a new generation of compact and robust femtosecond laser sources and inspires the development of fiber-based OPOs [7]. An OPOs pumped by a fiber laser, which has a high average power, efficiency, and environmental stability, is suitable to generate tunable and powerful ultrashort pulses. The first Yb-fiber-laser pumped OPO offering substantial power was reported by Lamour *et al.* [8], producing the highest pulse energy (72 nJ) obtained from a free-space resonator design. Recently, a Yb-fiber-laser-pumped, picosecond parametric oscillator, together with intracavity SHG tunable across 752 nm ~ 860 nm, was reported [9]. A femtosecond OPO based on LiB_3O_5 pumped by a frequency-doubled Yb-fiber amplifier at 525 nm provided signal tuning over 780 nm ~ 940 nm with more than 250 mW and idler tuning over 1190–1630 nm with more than 300 mW [10]. These ultrashort OPOs pumped by high-power ultrafast fiber lasers near 1 μm with intracavity frequency doubling and mixing, are able to provide the spectral range as that of Ti:sapphire lasers but are more robust and economical, together with higher output power [8–10]. As a result, extending the tunable wavelength range of a fiber laser-based OPO is an important and interesting topic for this technology.

In this Letter, we demonstrate the highly efficient generation of a widely tunable femtosecond pulses, red and near-infrared, from intracavity SHG and SFG in $\beta-BaB_2O_4$ (BBO) of an OPO, based on a 5% MgO-doped PPLN (MgO:PPLN) and infrared signal, and idler pulses directly obtained from an OPO. Owing to the high nonlinear gain in both PPLN and BBO, we achieve an average power of 470 mW at 23.5% conversion efficiency tuning across 716 nm ~ 970 nm for SHG, and 372 mW at 18.6% conversion efficiency tuning across 610 nm ~ 668 nm for SFG. Moreover, we obtain an average power of 694 mW average power for a 4.1 W pump, representing a 16.9% conversion efficiency for maximum SFG output at 615 nm. The SFG and SHG act as a signal output loss caused by the nonlinear process with hardly any affect on the stability of the original OPO.

The configuration of the femtosecond OPO is shown in Fig. 1. A homemade high-power Yb large-mode-area photonics crystal fiber (PCF) femtoseocond laser operating at a repetition rate of 51 MHz is used as the pump source. Its central wavelength is 1040 nm with an FWHM

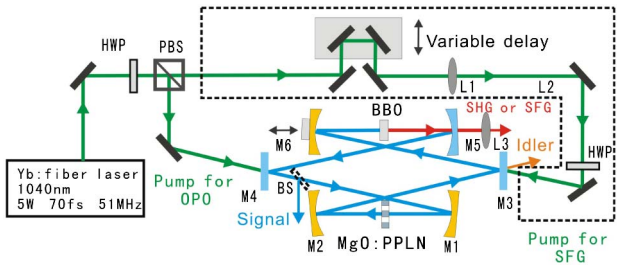

Fig. 1. Experimental setup of intracavity SHG and SFG in MgO:PPLN OPO. M1–M6, mirrors; L1–L3, lenses; HWP, half-wave plate; PBS, polarizing beam-splitter; BS, beam-splitter.

of 40 nm, and pulse duration of 70 fs. The nonlinear crystal for the OPO is a 1 mm long, 8.5 mm wide, 5% MgO: PPLN. In the experiment, the crystal is housed in an oven maintained at 80°C in order to avoid the photorefractive effect. The crystal contains seven gratings with periods ranging from 28.5 to 31.5 μm, in steps of 0.5 μm.

The OPO cavity is a bifocal ring, comprised of four concave and two plane mirrors. In order to enhance the intracavity nonlinear efficiency, the OPO has no output when operating for intracavity SHG and SFG. Gold-coated concave mirrors M1 and M2, with $r = 150$ mm, provide the focus for the OPO crystal, whereas mirrors M5 and M6, with $r = 100$ mm, allow focusing into the SHG or SFG crystal. M5 is an SHG or SFG output mirror, which is 99% reflective over 1400 nm ~ 2100 nm and 95% transmittive over 600 nm ~ 1000 nm, SHG or SFG is output through M5 and collimated by lens L3, M3, and M4 are dichroic pump mirrors, which are 99% reflective over 1400 nm ~ 2100 nm, 95% transmittive for the pump wavelength at 1.04 μm and highly transmittive for at idler wavelength. The crystal faces are AR-coated over 1000 nm ~ 1100 nm ($R < 1\%$) and 1420 nm ~ 2000 nm ($R < 1.5\%$). The crystal length is chosen to be 1 mm considering group-velocity mismatch (GVM). A BBO crystal is used for the SHG or SFG because of the weak dependence of the phase matching angle on the wavelength and small GVM in the near infrared region [11].

In order to characterize the OPO's spectral coverage, we tune the cavity length of the OPO with seven grating periods of the PPLN crystal. First, we obtain the signal by inserting a BS (beam splitter) as the output coupler. The signal and idler output powers of the OPO for different wavelengths are shown in Fig. 2(a). The maximum signal output power is 374 mW at 1502 nm corresponding to an 18.7% conversion efficiency, and the autocorrelation duration is 202 fs [Fig. 2(b)], corresponding to a 144 fs duration. The calculated transform-limit duration is about 90 fs. The duration is larger than the pump laser, mainly because of the GVM in the PPLN crystal. The idler power is measured at the back of M3. The spectra of the signal and idler pulses are shown in Figs. 2(c) and 2(d), respectively. The signal and idler spectra are continuously tuned from 1450 to 2200 nm and 2250 to 4000 nm, respectively, by changing the PPLN grating and the cavity length. The spectrum is noisy at 2200 nm, which is due to the instability of the OPO at degeneracy [12].

For the SHG and SFG processes, the BS output coupler is removed to enhance the intracavity power. The second harmonic (SH) signal is obtained simply by inserting the BBO crystal in the cavity. The BBO crystal is 2 mm thick, cut at $\theta = 23.2°$ for type I interaction. The crystal faces are AR-coated centered at 1.06 μm ($R < 1\%$). The SH of the signal is obtained simply by adjusting the cavity length and crystal angle. The tuning range of the SHG is 716–970 nm as shown in Fig. 3(a), and the wavelength limitation is mainly due to the reflection bandwidth of the mirrors. Figure 3(b) shows the dependence of SHG power on the wavelength at a fixed pump power of 2 W. The maximum output power is 470 mW with a 165 fs pulse duration [inset of Fig. 3(b)] and 12 nm spectrum width at 757 nm, corresponding to a time-bandwidth product of $\Delta\upsilon\Delta\tau \sim 1$. The net conversion efficiency is 23.5% for SH and the total efficiency including the idler is 35.2%. The SH power is above 200 mW over 716–850 nm, and above 100 mW at 970 nm.

In the case of SFG, an additional pump beam is used to overlap the intracavity signal beam instead of the residual pump light as before [13]. In order to get maximum SFG output, a half-wave plate (HWP) and a polarizing beam-splitter (PBS) are used to distribute the pump power for the OPO and SFG, and a second HWP is used to control the pump polarization for SFG phase-matching (Fig. 1). The additional pump beam is mode-matched with the oscillating signal beam by L1 ($f = 200$ mm) and L2 ($f = 100$ mm). In the time domain. the pump pulses are synchronized with the oscillating signal pulses in the crystal by adjusting the delay line.

The alignment of the SFG is performed from the SHG configuration simply by rotating the BBO a few degrees. The pump beam for SFG is adjusted to coincide with the signal beam line, and the SFG output is easily observed by scanning the delay line. At the optimum angle of SFG, only a few milliwatt of SH output remains. In a previous report [2], residual pump light from the OPO is used for intracavity SFG, and so the pump light is depleted in both parametric and SFG crystals. The output behavior of the OPO becomes complicated

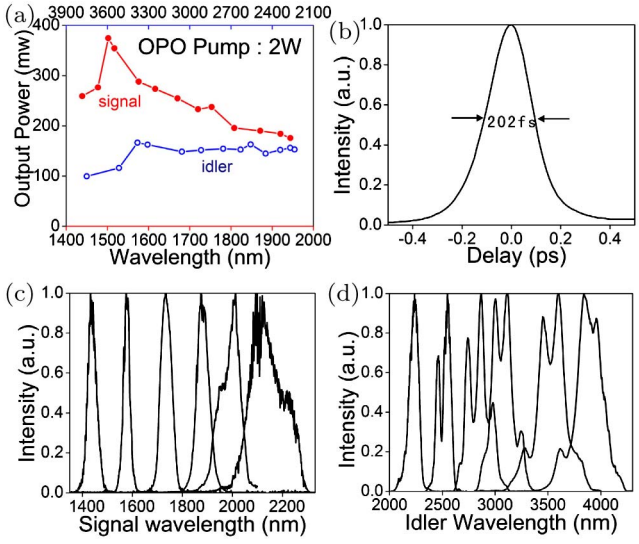

Fig. 2. (a) Output powers of the signal and idler, (b) autocorrelation of signal at 1514 nm, (c) spectrum tuning of the signal from 1450 to 2200 nm, and (d) spectrum tuning of the idler from 2250 to 4000 nm.

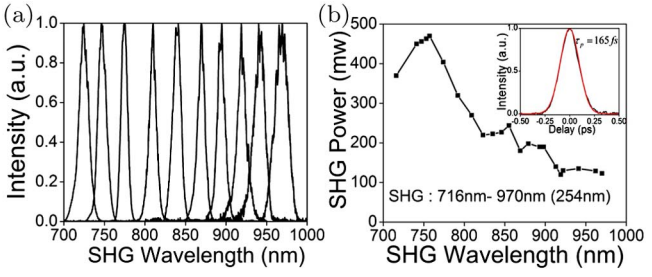

Fig. 3. (a) Spectrum tuning of the intracavity SHG from 716 to 970 nm and (b) dependence of output power of intracavity SHG on wavelength. Inset: autocorrelation of SHG signal at 757 nm.

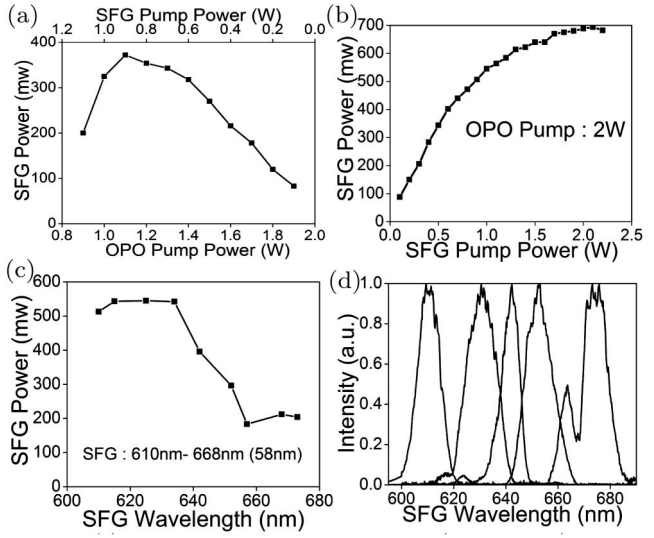

Fig. 4. (a) Dependence of SFG (at 615 nm) output power on the OPO and SFG pump powers, at a fixed total input power of 2 W, (b) SFG (at 615 nm) power with an increase of SFG pump power at a fixed OPO pump power of 2 W, (c) SFG power dependence on wavelength at a fixed OPO pump power of 2 W and SFG pump power of 1 W, and (d) spectrum tuning of SFG from 610 to 668 nm.

because of its dependence on the degree of pump light depletion in both crystals. Using an additional pump light makes the behavior of the OPO simple and stable, and it is easy to obtain an optimum SFG. The distribution ratio of the OPO is a key parameter of the SFG power. If the ratio of the OPO pump light is too small, the intracavity signal power will be too low or unable to maintain the oscillation. If the ratio of the SFG pump light power is too small, the nonlinear interaction of the fundamental and signal will also be inefficient. So, it has an optimum value for the maximum output power of SFG. Figure 4(a) shows the dependence of the SFG output power on the distribution at a fixed total pump power of 2 W. The OPO starts oscillating at 868 mW, which is much higher than the threshold (287 mW) without the SFG pump in. This is because the SFG increases the loss of the cavity. So, the SFG power rises with the increase of OPO pump power, and reaches a maximum output of 372 mW corresponding to an 18.6% conversion efficiency at an OPO pump power of 1.1 W. With further increases in the OPO pump power, the SFG power decreases. Figure 4(b) shows the dependence of the SFG power on the SFG pump power at a fixed OPO pump power of 2 W. Initially, the SFG power grows with the SFG pump power linearly, and then tends to be saturated. The maximum SFG power is 694 mW at a SFG pump power of 2.1 W, corresponding to a 16.9% conversion efficiency. It is because the increase of the SFG power indicates more intracavity signal depletion, and the SFG power stops increasing when it reaches a balance. The tuning property of the SFG is also recorded by tuning the cavity length of the OPO with seven grating periods of the PPLN crystal. For optimum SFG output power, a slight phase-matching angle rotation of the BBO is also performed. Figure 4(c) shows the SFG power at a fixed OPO pump power of 2 W and an SFG pump power of 1 W, the maximum output power being 545 mW corresponding to an 18.1% conversion efficiency. Figure 4(d) shows the spectrum tuning coverage from 610 to 668 nm continuously. An abrupt drop by a factor of 2 for the SFG intensity at wavelengths around 640 nm is mainly caused by the decreasing signal intensity due to the increasing GVM between the signal and pump, which reduce the intracavity signal power and increase the duration of signal, which both reduces the intensity of the signal. The temporal walk-off between the signal and SFG in the 2 mm BBO is about 230 fs, and the temporal walk-off between the pump and signal is 30 fs, which is relatively small, and so the duration of the SFG is estimated to be about 300 fs.

In summary, we have demonstrated a femtosecond source tunable across 610–668 nm and 716–970 nm based on intracavity SHG and SFG in a MgO:PPLN OPO, together with signal and idler tuning in the near- and mid-infrared regions. We have obtained 470 mW of power for a 2 W Yb:fiber laser pump with a 23.5% conversion efficiency for SHG and 372 mW with a 18.6% conversion efficiency for SFG. Future work will be focused on increasing the output power and extending the operating wavelength of fiber femtosecond laser based OPOs. A double pumped OPO setup and an additional SHG process can be applied to obtain the high average power tunable ultraviolent femtosecond pulse. It can be expected that these techniques will lead to a feasible scenario in many applications.

This research is supported by the National Basic Research Program of China (Grant 2011CB808101 and 2010CB327604) and the National Natural Science Foundation of China (Grant 61078028, 61205131, and 11274239).

References

1. M. Jurna, J. P. Korterik, H. L. Offerhaus, and C. Otto, Appl. Phys. Lett. **89**, 251116 (2006).
2. A. Zumbusch, G. R. Holtom, and X. S. Xie, Phys. Rev. Lett. **82**, 4142 (1999).
3. A. Shirakawa, H. W. Mao, and T. Kobayashi, Opt. Commun. **123**, 121 (1996).
4. A. Esteban-Martin, O. Kokabee, and M. Ebrahim-Zadeh, Opt. Lett. **33**, 2650 (2008).
5. K. C. Burr, C. L. Tang, M. A. Arbore, and M. M. Fejer, Appl. Phys. Lett. **70**, 3341 (1997).
6. K. Koch, G. T. Moore, and E. C. Cheung, J. Opt. Soc. Am. B **12**, 2268 (1995).
7. J. Limpert, F. Roser, T. Schreiber, and A. Tunnermann, IEEE J. Sel. Top. Quantum Electron. **12**, 233 (2006).
8. T. P. Lamour, L. Kornaszewski, J. H. Sun, and D. T. Reid, Opt. Express **17**, 14229 (2009).
9. S. Chaitanya Kumar, O. Kimmelma, and M. Ebrahim-Zadeh, Opt. Lett. **37**, 1577 (2012).
10. C. Cleff, J. Epping, P. Gross, and C. Fallnich, Appl. Phys. B **103**, 795 (2011).
11. R. J. Ellingson and C. L. Tang, Opt. Lett. **18**, 438 (1993).
12. J. Falk, IEEE J. Quantum Electron. **7**, 230 (1971).
13. A. Shirakawa, H. W. Mao, and T. Kobayashi, Opt. Commun. **123**, 121 (1996).